MOLECULAR AND CELLULAR BIOLOGY, Jan. 1993, p. 217–227
0270-7306/93/010217-11$02.00/0

Vol. 13, No. 1

A *Drosophila* Homolog of Bovine *smg* p25a GDP Dissociation Inhibitor Undergoes a Shift in Isoelectric Point in the Developmental Mutant *quartet*

JOSEPH E. ZAHNER AND CLARISSA M. CHENEY*

Department of Genetics, Box 8232, Washington University School of Medicine, 4566 Scott Avenue, St. Louis, Missouri 63110

Received 21 January 1992/Returned for modification 3 March 1992/Accepted 3 October 1992

The *Drosophila* developmental mutation *quartet* causes late larval lethality and small imaginal discs and, when expressed in the adult female, has a lethal effect on early embryogenesis. These developmental defects are associated with mitotic defects, which include a low mitotic index in larval brains and incomplete separation of chromosomes in mitosis in the early embryo. *quartet* mutations also have a biochemical effect, i.e., a basic shift in isoelectric point in three proteins. We have purified one of these proteins, raised an antibody to it, and isolated and sequenced its cDNA. At the amino acid level, the sequence shows 68% identity and 81% similarity to bovine *smg* p25a GDP dissociation inhibitor (GDI), a regulator of *ras*-like small GTPases of the *rab/SEC4/YPT1* subfamily. The correlation between a basic shift in isoelectric point in *Drosophila* GDI in *quartet* mutant tissue and the *quartet* developmental phenotype raises the possibility that a posttranslational modification of GDI is necessary for its function and that GDI function is essential for development.

Small GTPases have been shown to play critical roles in regulating several fundamental cell processes, including signal transduction, protein synthesis, and vesicular transport (for reviews, see references 7, 8, 20, and 42). At least three classes of regulatory proteins are involved in the control of small GTPases: (i) GTPase-activating proteins, which activate GTP hydrolysis; (ii) guanine nucleotide-releasing proteins, which are essential for the release of GTP and GDP from GTPases; and (iii) GDP dissociation inhibitors (GDIs), which prevent the dissociation of GDP from small GTPases. GTPase-activating proteins and guanine nucleotide-releasing proteins have been identified in genetically tractable systems. We present here the identification of a GDI gene in *Drosophila melanogaster*. This is the first report of a complete GDI sequence in a genetic model system. This GDI shows a shift in isoelectric point in the *Drosophila* developmental and mitotic mutant *quartet*. This discovery opens the way for genetic analysis of the functions of GDIs and their role in cellular processes and raises the possibility that a posttranslational modification of GDI is needed for its function.

The *Drosophila* developmental mutant *quartet* has a complex phenotype. Developmental defects in *quartet* animals involve late larval lethality, small imaginal discs, and reduced mitotic activity in larval brains (31, 32, 47). When expressed in the adult female, *quartet* mutations produce a maternal lethal effect on the embryo, with incomplete chromosome separation during early embryonic mitotic divisions (47). This constellation of phenotypic defects indicates that the *quartet* gene product is essential for development.

Together with these developmental defects, *quartet* has an interesting and unusual biochemical phenotype. In *quartet* homozygous animals, three abundant proteins undergo a change in overall charge, as evidenced by a basic shift in mobility on two-dimensional (2D) gels (13). Of 300 proteins which can be reproducibly distinguished on these high-resolution gels, only 3 of these are shifted in *quartet* tissue. Rigorous genetic tests have shown that this charge shift is due to mutation of only the *quartet* locus and not to mutations outside the *quartet* locus that may be linked to *quartet* (12). The severity of the developmental defects closely correlates with the amount of protein that is shifted. In severe *quartet* alleles, a larger portion of each affected protein is shifted to the more basic isoform. In mild *quartet* alleles, only a small portion of each affected protein is shifted to the more basic isoform. Finally, the charge shift and the *quartet* developmental defects are both temperature sensitive in a temperature-sensitive allele of *quartet* (11). These correlations between charge shift and *quartet* developmental defects indicate that the shifted proteins are intimately, perhaps causally, correlated with the developmental defects in *quartet* mutants. A working hypothesis connecting the *quartet* developmental phenotype with the biochemical phenotype is that the *quartet* locus codes for an enzyme which posttranslationally modifies three proteins. Mutations in *quartet* could destroy the activity of this enzyme and result in an altered charge in these proteins, which can then no longer function normally. Because the more basic isoform of each protein accumulates in *quartet* tissue, it is possible that this modification is an acidic modification. Alternatively, it could be that the wild-type *quartet* gene product removes a basic modification. The proteins shifted in the *quartet* phenotype could play important roles in development and may have to be posttranslationally modified to carry out these roles.

In this report, we describe the isolation of one of the *quartet*-shifted proteins and demonstrate that it is homologous to the bovine *smg* p25a GDI (28). Bovine GDI is a regulator of small GTPases of the *rab/YPT1/SEC4* family (38, 39). The conceptual translation of the *Drosophila* GDI sequence shows 68% identity and 81% similarity to the sequence of bovine *smg* p25a GDI. The correlation between the basic shift of the *Drosophila* GDI and the *quartet* developmental defects indicates that posttranslational modification of GDI could regulate its function.

* Corresponding author.

MATERIALS AND METHODS

Fly stocks. Fly stocks were maintained at 20°C, unless indicated otherwise, in plastic vials on standard cornmeal-molasses-agar medium with propionic acid added to inhibit mold. Fly embryos were obtained from a fly population facility maintained by the laboratory of S. C. R. Elgin, Department of Biology, Washington University. Ovaries for 1D and 2D gels were from Oregon-R flies or from *red* flies. *red* is the genetic background in which the *quarter*^{RW630} mutation was induced.

Buffers. Homogenization buffer consists of 0.1 M 2-(*N*-morpholino)ethanesulfonic acid (MES; pH 6.9), 5 mM ethylene glycol-bis(β-aminoethyl ether)-*N*,*N*,*N*′,*N*′-tetraacetic acid (EGTA), 0.9 M glycerol, 0.5 mM ATP, 10 mM sodium *p*-tosyl-L-arginine methyl ester, 1 mM phenylmethylsulfonyl fluoride, 0.2 mM dithiothreitol, and 0.05% NaN_3. DEAE buffer consists of 10 mM Tris · HCl (pH 8.0), 0.1 mM EGTA, 0.5 mM ATP, 0.2 mM dithiothreitol, 0.05 mM $MgCl_2$, and 0.05% NaN_3. Hydroxylapatite (HAP) buffer consists of 10 mM potassium phosphate (pH 7.0), 0.5 mM ATP, 0.02 mM dithiothreitol, and 0.05% NaN_3.

Protein $b_{6.1}$ isolation. All procedures were carried out at 4°C. Protein concentrations were measured by using the Bradford assay (9) with bovine serum albumin as the standard. This protocol for protein $b_{6.1}$ isolation (15) was based on the protocol of Wang and Spudich (46) for isolation of a 45-kDa, pI 6.0 protein from sea urchin embryos. The starting material was 0 to 24-h-old *Drosophila* embryos which were frozen at −70°C immediately after collection. A 100-g portion of frozen embryos was homogenized in 200 ml of homogenization buffer in an Osterizer Touch 'N' Pulse blender for two 30-s pulses on the liquify setting. Centrifugation at 20,000 × *g* for 60 min in the GSA rotor of a Sorvall RC2B centrifuge removed large particulate debris, such as vitelline membranes and yolk protein. The supernatant was then filtered through one layer of Nitex 180-μm mesh. The filtrate was dialyzed overnight into DEAE buffer with three changes of 2.5 liters each. In a typical run, a total of 800 to 900 mg of protein in 100 ml of DEAE buffer was loaded onto a DEAE-cellulose column (no. D-3764, microgranular; Sigma Chemical Co.) that was 33 cm high and 2.6 cm in diameter. After a 100-ml wash with DEAE buffer, a 0 to 0.3 M NaCl gradient in 520 ml was passed through the column. The flow rate was 30 ml/h, and 4-ml fractions were collected. Protein concentration was monitored by using an ISCO model UA-5 UV column monitor. Conductivity was measured with a YSI model 32 conductance meter. Fractions with conductivity corresponding to 0.14 to 0.15 M NaCl were pooled and concentrated. A 10-mg portion of protein in 1 ml was loaded onto a Sephadex G-100 (Pharmacia-LKB) column that was 84 cm high and 1.6 cm in diameter. The flow rate was 12 ml/h, and 1-ml fractions were collected. Carbonic anhydrase, bovine serum albumin, and cytochrome *c* were used to calibrate the column. The fractions containing 45- to 60-kDa proteins were pooled and dialyzed overnight into HAP buffer with three changes of 1 liter each. A 3-mg portion of protein in 5 to 10 ml was loaded onto a HAP column (BioGel-HTP; Bio-Rad) that was 5 cm high and 1.5 cm in diameter. Proteins were eluted with a 50-ml gradient of 0.01 to 0.5 M potassium phosphate (pH 7.0) at 12 ml/h. Fractions of 0.5 ml were collected. Protein $b_{6.1}$ eluted in the 0.22 to 0.24 M potassium phosphate fractions. From 100 g of embryos, approximately 80 μg of purified protein $b_{6.1}$ was isolated.

Antibodies to HAP protein $b_{6.1}$. Approximately 0.5 mg of HAP protein $b_{6.1}$ was loaded onto a sodium dodecyl sulfate (SDS)–10% polyacrylamide gel and separated electrophoretically. The major band was cut out and emulsified with 1 ml of RIBI adjuvant (RIBI ImmunoChem Research Inc., Hamilton, Mont.), and 200 μl was injected intraperitoneally into a mouse. This injection was repeated twice more at 10-day intervals. A total of six mice were subjected to this regimen. The sera were tested by Western immunoblotting to 1D and 2D blots of the G-100 purified protein and of total ovary proteins (22). Four mice showed a positive response. The antiserum from the mouse with the strongest response will be referred to as anti-$b_{6.1}$. For detection of antigen on Western blots, anti-$b_{6.1}$ was routinely used at a dilution of 1/1,000. When anti-$b_{6.1}$ was used to immunofluorescently stain *Drosophila* embryos, only a general cytoplasmic staining, indistinguishable from background, was observed.

Antibodies to GST.DmCp fusion protein. cDNA insert was purified from λgt11.DmC and ligated into a pGEX1 vector (Pharmacia-LKB) to give the plasmid pGEX.DmC. This produced a glutathione-*S*-transferase fusion protein (GST.DmCp). Total expressed pGEX.DmC and bacterial proteins were loaded onto a 50-ml glutathione-agarose column (sulfur linkage; Sigma Chemical Co.) and eluted with a 50-ml gradient of 0 to 50 mM reduced glutathione in 100 mM Tris HCl (pH 8.0) (40). Proteins in the largest protein peak eluted from this column were separated electrophoretically on a 1D gel. A test strip from this gel was blotted and reacted with anti-$b_{6.1}$ to ascertain the exact position of GST-DmCp. A 150- to 250-μg portion of this protein was cut from the 1D gel, suspended in 1 ml of RIBI adjuvant, and injected subcutaneously into a rabbit. This injection was repeated twice more at 10-day intervals. Antibodies were affinity purified from whole-rabbit serum by using a column made of glutathione-agarose beads to which proteins from pGEX.DmC-infected bacteria had been bound. The whole-rabbit antiserum was loaded onto the column. After being washed, bound antibodies were eluted with 100 mM diethylamine (pH 11.6) and immediately neutralized (22). This antibody will be referred to as anti-GST.DmCp. All Western blotting experiments reported here with anti-GST.DmCp were performed with this affinity-purified antibody at a dilution of 1/50. When anti-GST.DmCp was used to immunofluorescently stain *Drosophila* embryos, only a general cytoplasmic staining, indistinguishable from background, was observed.

Antibodies to phosphotyrosine. A monoclonal mouse anti-phosphotyrosine antibody (no. P-3300, clone PT-66; Sigma) was used at dilutions ranging from 1/50 to 1/2,000. Another mouse monoclonal anti-phosphotyrosine antibody (no. 1083-155, clone 1G2; Boehringer Mannheim) was used at dilutions of 1/78 to 1/1,000. Human lymphocytes were used as a positive control.

Secondary antibodies. Mouse primary antibodies were detected on Western blots by using a 1/1,000 dilution of an alkaline phosphatase-conjugated anti-mouse immunoglobulin G made in goats (no. A5153; Sigma). The primary antibody and secondary antibody complex was detected by formation of a colored product from Nitro Blue tetrazolium and 5-bromo-4-chloro-3-indolyl phosphate. Rabbit primary antibodies were detected on Western blots by using a 1/5,000 dilution of an alkaline phosphatase-conjugated anti-rabbit immunoglobulin G made in goats (no. 5373B; Promega).

Electrophoretic techniques. 1D gel analysis of proteins was performed with 10% polyacrylamide gels except when noted (25). Gels were stained with Coomassie brilliant blue R. 2D gel analysis was performed by the method of O'Farrell (29)

as modified by Cheney and Shearn (14). Unless stated otherwise, proteins analyzed on the gels were from adult *Drosophila* ovaries. Ovaries were dissected in insect Ringer's solution and prepared for 2D gel analysis as described by Cheney and Shearn (14). For 1D gel analysis, dissected ovaries were lysed by freezing and thawing in the hypotonic lysis buffer of Fyrberg and Donady (19). Then 5× SDS sample buffer was added to bring the final concentration of the sample to 1× SDS sample buffer. DNA was analyzed by electrophoresis in 1% agarose gels, using standard techniques (36).

Blots. Western blots of 1D and 2D protein gels were performed in a Hoefer TE 50 Western electroblotting apparatus as specified by the manufacturer. For all protein blots, Immobilon-P membrane (Millipore) was used. DNA separated in agarose gels was transferred to Nytran nylon membrane (pore size, 0.45 μm; Schleicher & Schuell) by the procedure of Southern (41). Specific nucleotide sequences on Southern blots were detected by hybridization with double-stranded DNA probe that had been labeled with [^{32}P]ATP by the random-primer method of labeling. Southern blots were hybridized overnight at 68°C in 6× SSC (1× SSC is 0.15 M NaCl plus 0.015 M sodium citrate)–5× Denhardt's solution–0.5% SDS–20 μg of salmon testis DNA per ml. Washing was done in 0.1× SSC–0.1% SDS at 68°C.

Library screening. (i) cDNA libraries. The *Drosophila* ovary λgt11 cDNA expression library of P. Sullivan, D. Joseph, and L. Kalfayan was screened with anti-$b_{6.1}$, using standard techniques (36). This library was made from ovarian mRNA by oligo(dT) priming and cloned into λgt11. One positive clone was identified from 300,000 plaques screened.

The adult female λgt10 cDNA library of Kauvar and Kornberg was screened with the cDNA insert from λgt11.DmC, using standard techniques (36). Five positive clones were identified from 125,000 plaques screened. These five clones turned out to have identical inserts, and so four of these clones were discarded and one (λgt10.Dm237) was kept for further analysis.

(ii) Genomic library. The *Drosophila* Oregon-R EMBL4 genomic library of Pirrotta was screened. Two positive (λEMBL4.DmA and λEMBL4.DmD) clones were identified from 60,000 plaques screened.

Sequencing. (i) Nucleic acids. Sequencing was done by the dideoxynucleotide-chain termination method (37) with the Sequenase kit (U.S. Biochemical Corp.). For sequencing, cDNA inserts were subcloned into a pBluescript SK$^-$ vector (Stratagene) and M13 universal primers were used. Internal sequences were determined either by using an oligonucleotide primer to an internal sequence or by using the Erase-a-Base kit (Promega). Both strands of λgt11.DmC and λgt10.Dm237 were sequenced. DNA database searches were done by using the FASTA program (30).

(ii) Proteins. HAP protein $b_{6.1}$ was cleaved with CNBr (10). The peptides were separated by high-pressure liquid chromatography on a Brownlee Rp300 aquapure bore C18 column (2.1 mm by 22 cm). Selected peptides were sequenced by the Edman reaction (phenylisothiocyanate degradation). Peptide sequencing was done by the Protein Chemistry Facility of the Department of Biochemistry and Molecular Biophysics, Washington University.

Partial proteolytic digests. Partial proteolytic digests were performed by the procedure of Cleveland et al. (15) with *Staphylococcus aureus* V8 endoproteinase Glu-C (Boehringer Mannheim) at the indicated concentrations. Peptide digests were analyzed by SDS-gel electrophoresis on 15% acrylamide gels. Peptides were visualized by staining with a silver stain (Hi Ho Silver stain; Accurate Chemical and Scientific Company).

Phosphatase treatment of dGDI. dGDI (10 pmol) was digested with 9.75 U of alkaline phosphatase (no. P-7915; Sigma) in 100 mM diethanolamine (pH 9.8)–5 mM $MgCl_2$ at 37°C for 1 h. Urea was added to 7 M, and then 1.5 volumes of O'Farrell solution A were added (29). The sample was then analyzed by 2D gel electrophoresis. Immediately before the treated protein was loaded onto the isoelectric focusing gel, 10 pmol of untreated dGDI was added to the sample to act as an internal gel marker for precise comparison of isoelectric points between treated and untreated dGDI. The activity of the phosphatase was checked by a colorimetric phosphatase assay with *p*-nitrophenyl phosphate as the substrate.

In situ hybridization. Third-instar larval salivary glands were dissected, fixed, and squashed by the method of Johnson-Schlitz and Lim (23). Biotin-labeled DNA probe was made by the procedure of Feinberg and Vogelstein (17) with biotinylated ATP and then hybridized to polytene chromosomes by using method 3 of Langer-Safer et al. (27). Hybridized probe was detected by its reaction with streptavidin-peroxidase (ENZO Biochem) followed by peroxidase staining with diaminobenzidine.

In vitro transcription and in vitro translation. An in vitro *Drosophila* GDI transcript was made by transcribing pBS.237, which has the λgt10.Dm237 cDNA insert in pBluescript SK$^-$. Transcription was done with the Stratagene in vitro transcription kit (no. 200340) and T7 polymerase as specified by the manufacturer. A control reaction with T3 polymerase was also carried out. A small amount (~400 μCi/ml) of [^{32}P]UTP was added to each reaction mixture as a tracer to monitor the synthesis of RNA. To increase translational efficiency, 0.8 mM P^1-5′-(7-methyl)-guanosine-P^3-ATP was included in each transcription reaction. The transcript was treated with RNase-free DNase, separated from unincorporated nucleotides by using a Pharmacia G-25 nick column, extracted with phenol-chloroform, and precipitated with ethanol. After precipitation, the RNA was dissolved in diethylpyrocarbonate-treated water, and the RNA concentration was estimated by spectrophotometric analysis at 260 nm.

In vitro translation was performed by using a nuclease-treated rabbit reticulocyte lysate kit (no. L4960; Promega) as specified by the manufacturer. Four reactions were performed: (i) translation of the pBS.237 T7 polymerase transcript at 29 μg of RNA per ml; (ii) translation of the pBS.237 T3 transcript at 25 μg of RNA per ml; (iii) translation of luciferase mRNA (the positive control supplied with the kit); and (iv) translation with no added RNA. The synthesis of protein was monitored by adding [^{35}S]methionine (final concentration, 800 μCi/ml) to each translation. The translation products were digested with RNase A and DNase I. Crystalline urea was added to 8 M, an equal volume of O'Farrell solution A (29) was added, and the samples were analyzed by 2D gel electrophoresis. To determine clearly which isoform of *Drosophila* GDI was made during in vitro translation, several *quartet* ovaries, which contained both GDI isoforms, were coloaded with the T7 transcript translation product. The *quartet* ovaries were from *quartet*^{RW630} homozygous adult female flies that had been kept at 27°C for 2 days.

The 2D gels of the translation products were blotted to an Immobilon-P membrane and stained for *Drosophila* GDI with a mouse anti-native protein $b_{6.1}$ antibody at a dilution of 1/1,000. The stained blots were dried and autoradiographed.

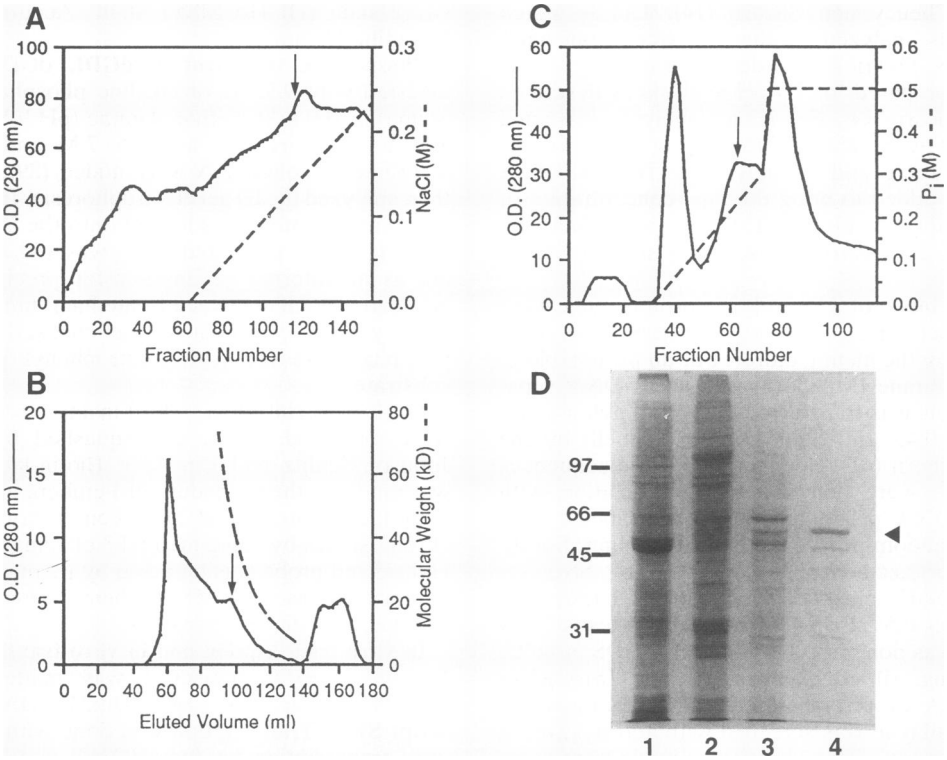

FIG. 1. Purification of protein $b_{6.1}$. (A) DEAE-cellulose column chromatographic distribution of embryo proteins. Embryos were homogenized, and proteins from these embryos were applied to a DEAE-cellulose column and eluted with an NaCl gradient. The arrow indicates the fraction with the most protein $b_{6.1}$ as assayed by 2D gel electrophoresis. (B) G-100 Sephadex column chromatographic distribution of pooled DEAE-fractionated embryo proteins. Embryo proteins in the fraction marked by an arrow in panel A and its flanking fractions were pooled and applied to a G-100 Sephadex molecular sieve column. The mobilities of molecular weight markers on this column are indicated by the dotted line. The arrow indicates the fraction with the most protein $b_{6.1}$ as assayed by 2D gel electrophoresis. (C) HAP column chromatographic distribution of pooled G-100-fractionated embryo proteins. The fraction marked by an arrow in panel B and its flanking fractions were pooled and applied to a HAP column. Proteins were eluted with a potassium phosphate gradient. The arrow indicates the fraction with the most protein $b_{6.1}$ as assayed by 2D gel electrophoresis. (D) Electrophoretic analysis of embryo proteins at different steps in the protein purification. Embryo proteins in column fractions indicated by arrows in panels A, B, and C were concentrated and subjected to 1D gel electrophoresis. Proteins were visualized in the gel by staining with Coomassie brilliant blue. Positions of molecular weight markers are indicated on the left of the gel. Lanes: 1, proteins in an aliquot of embryo homogenate before loading onto the DEAE-cellulose column in panel A; 2, proteins in the DEAE fraction indicated by an arrow in panel A and in the flanking fractions; 3, proteins in the G-100 fraction indicated by an arrow in panel B and in the flanking fractions; 4, proteins in the HAP fraction indicated by an arrow in panel C and in the flanking fractions. The 50-kDa protein marked by an arrowhead is protein $b_{6.1}$ as assayed by 2D gel electrophoresis. O.D., optical density.

To ensure accurate alignment of the stained blot and the autoradiographic image, the blots were taped to a firm support and two light-emitting markers were placed asymmetrically on this support. The image of the markers on the exposed film could then be easily and accurately lined up with the markers positioned on the support and hence allowed careful assessment of which isoform of *Drosophila* GDI was made.

Nucleotide sequence accession number. The GenBank accession number of dGDI is L03209.

RESULTS

Purification of protein $b_{6.1}$. A chromatographic isolation protocol was devised to purify protein $b_{6.1}$, one of three proteins which undergo a basic shift in isoelectric point in *quartet* mutants (11–13). Since protein $b_{6.1}$ is well resolved from neighboring proteins on 2D gels, it can be unambiguously identified by its 2D gel mobility. Therefore, the purification of protein $b_{6.1}$ was monitored by 2D gel analysis of chromatographically separated *Drosophila* embryo proteins. The presence of a protein with the same molecular weight and isoelectric point as protein $b_{6.1}$ on 2D gels of column fractions was taken to indicate that protein $b_{6.1}$ was present in those fractions. For final confirmation, peptide maps of the purified protein were compared with peptide maps of protein $b_{6.1}$ that had been cut from 2D gels of ovary proteins.

The purification scheme involved three chromatographic separations. Embryos were homogenized, and the homogenate was centrifuged to remove large particulate debris. The supernatant was loaded onto a DEAE ion-exchange column, and bound proteins were eluted with a salt gradient (Fig. 1A). Column fractions containing protein $b_{6.1}$ were pooled, concentrated, and loaded onto a Sephadex G-100 molecular sieve column (Fig. 1B). G-100 fractions containing protein $b_{6.1}$ were pooled, concentrated and loaded onto a HAP column (Fig. 1C). HAP fractions containing protein $b_{6.1}$ were pooled. This purification scheme gave an increasing level of purity with each step (Fig. 1D), resulting in a fraction that contained one major and several minor proteins (Fig. 1D, lane 4). The major protein had the same molecular weight as protein $b_{6.1}$ and will be referred to as HAP protein

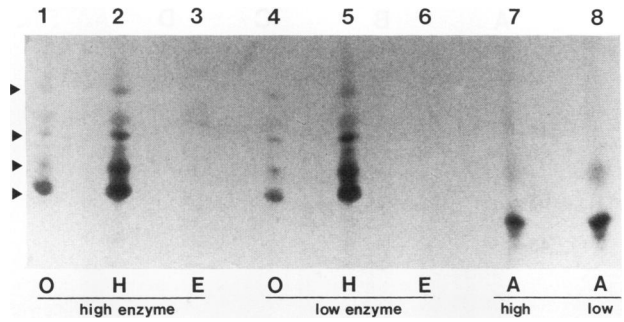

FIG. 2. HAP-purified protein $b_{6.1}$ is the same protein as ovary protein $b_{6.1}$ cut from 2D gels. Proteins were loaded onto a 1D 15% acrylamide gel together with *S. aureus* endoproteinase Glu-C and partially cleaved by the procedure of Cleveland et al. (15). The gel was stained with a silver stain. Arrowheads on the left side of the gel mark peptides found in protein $b_{6.1}$ digests. From top to bottom, the molecular masses of these peptides are 21.1, 19.4, 18.5, and 17.7 kDa. Lane 1, peptide digest of protein $b_{6.1}$ spots cut out from 2D gels of ovary proteins (O). Spots from three gels, representing proteins from 20 to 30 ovaries, were loaded into this lane together with 1 μg of enzyme. Lane 2, peptide digest of HAP protein $b_{6.1}$ (H). The 50-kDa protein band indicated by an arrow in Fig. 1D, lane 4, was cut out and loaded into this lane together with 1 μg of enzyme. The peptide pattern in this lane is identical to the pattern in lane 1, indicating that ovary protein $b_{6.1}$ and HAP-purified protein $b_{6.1}$ are the same protein. Lane 3, 1 μg of enzyme alone (E). Only one band is observed, indicating that all other bands observed in lanes 1 and 2 are from the loaded fly protein and are not breakdown products of the enzyme itself. Lane 4, peptide digest of protein $b_{6.1}$ spots cut out from 2D gels of ovary proteins (O). Spots from three gels, representing proteins in 20 to 30 ovaries, were loaded into this lane together with 0.2 μg of enzyme. Lane 5, peptide digest of HAP-purified protein $b_{6.1}$ (H). The 50-kDa protein band indicated by an arrow in Fig. 1D, lane 4, was cut out and loaded into this lane together with 0.2 μg of enzyme. The pattern of cleavage products in this lane is identical to that in lane 4, indicating that ovary protein $b_{6.1}$ and HAP protein $b_{6.1}$ are the same protein. Lane 6, 0.2 μg of enzyme alone (E). Only one band is observed, indicating that all other bands in lanes 4 and 5 are from the loaded fly protein and are not breakdown products of the enzyme itself. Lanes 7 and 8, peptide digests of actin (A). Actin spots from three 2D gels of ovary proteins were cut out and loaded into each lane together with 1 μg (lane 7) or 0.2 μg (lane 8) of enzyme. Actin was identified on 2D gels by molecular mass, isoelectric point, and quantity. This actin peptide pattern is very different from that of protein $b_{6.1}$, confirming that this peptide analysis technique clearly has the capability to distinguish different protein species.

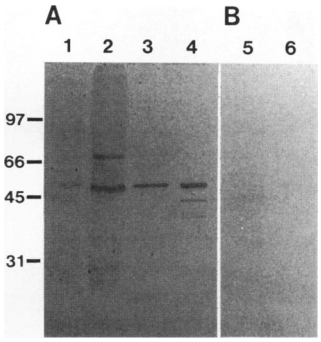

FIG. 3. Anti-$b_{6.1}$ reacts specifically with protein $b_{6.1}$. (A) Proteins from different stages of the protein $b_{6.1}$ purification procedure were separated by 1D SDS-gel electrophoresis and blotted onto an Immobilon-P membrane. Part of the blot was reacted with anti-$b_{6.1}$ and with an alkaline phosphatase-conjugated goat anti-mouse secondary antibody and stained for alkaline phosphatase. (B) Another part of the blot was reacted with secondary antibody alone and stained for alkaline phosphatase. Positions of molecular mass markers are indicated to the left of the figure. Lane 1, proteins from homogenized ovaries. Lane 2, proteins in DEAE-cellulose fractions marked by an arrow in Fig. 1A and in flanking fractions. Lane 3, proteins in G-100–Sephadex fractions marked by an arrow in Fig. 1B and in flanking fractions. Lane 4, proteins in HAP fractions marked by an arrow in Fig. 1C and in flanking fractions. Note that anti-$b_{6.1}$ reacts with a band at 50 kDa in lanes 1 to 4 and that the relative amount of this band increases during the purification procedure. The reaction with the 70-kDa band in lane 2 was significantly weaker than the reaction with the 50-kDa band and was not always present. The lower-molecular-mass bands in lane 4 which showed weak reaction with the antiserum could be degradation products of HAP protein $b_{6.1}$. Lane 5, proteins in homogenized ovaries, reacted with secondary antibody alone. Lane 6, proteins in HAP fractions marked by an arrow in Fig. 1C and in flanking fractions, reacted with secondary antibody alone. No staining is observed in lanes 5 and 6 at 50 kDa, indicating that the 50-kDa band that stains in lanes 1 to 4 reacts with anti-$b_{6.1}$ and not to the secondary antibody.

$b_{6.1}$. On 2D gels, HAP protein $b_{6.1}$ comigrated with ovary protein $b_{6.1}$, indicating that these proteins also have the same isoelectric point.

To provide further evidence that HAP protein $b_{6.1}$ was the same protein as ovary protein $b_{6.1}$, we compared peptide maps of these two proteins. By using the technique of Cleveland et al. (15), HAP protein $b_{6.1}$ and ovary protein $b_{6.1}$ were partially digested with protease and the digest products were separated electrophoretically. These two proteins gave identical patterns of proteolytic peptide fragments, indicating that HAP protein $b_{6.1}$ has the same distribution of proteolytic cleavage sites as ovary protein $b_{6.1}$ does (Fig. 2, lanes 1 to 6). Two different protease concentrations gave this result. Digests of a protein unrelated to protein $b_{6.1}$ gave a different pattern of peptide fragments, indicating that this technique is capable of distinguishing different proteins (Fig. 2, lanes 7 and 8). Because HAP protein $b_{6.1}$ and ovary protein $b_{6.1}$ have identical peptide maps, we conclude that HAP protein $b_{6.1}$ is the same protein as ovary protein $b_{6.1}$.

Antiserum to HAP protein $b_{6.1}$. With the goal of cloning the gene for protein $b_{6.1}$, we raised an antiserum to HAP protein $b_{6.1}$ by cutting the 50-kDa band out of a 1D gel of HAP protein $b_{6.1}$ and injecting this gel piece into a mouse. The antiserum (anti-$b_{6.1}$) produced in response to this antigen reacted reproducibly and strongly with a 50-kDa protein on 1D Western blots of ovary and embryo proteins (Fig. 3). On a 2D Western blot of ovary proteins, anti-$b_{6.1}$ reacted only with protein $b_{6.1}$ (Fig. 4). These data indicate that anti-$b_{6.1}$ reacts with protein $b_{6.1}$.

Isolation of a cDNA clone encoding protein $b_{6.1}$. A *Drosophila* ovary cDNA λgt11 expression library was screened for plaques producing fusion proteins which react with anti-$b_{6.1}$. Of 300,000 clones screened, 1 (λgt11.DmC) showed reproducible reactivity with anti-$b_{6.1}$ (Fig. 5). λgt11.DmC contains 0.9 kb of DNA and encodes a 150-kDa β-galactosidase fusion protein (β-gal.DmCp). The finding that anti-$b_{6.1}$ reacts with protein $b_{6.1}$ and also with β-gal.DmCp indicates that protein $b_{6.1}$ and β-gal.DmCp have at least one epitope in common.

To provide additional data that the cDNA in λgt11.DmC codes for a protein which shares an epitope with HAP protein $b_{6.1}$, we ligated the cDNA insert from λgt11.DmC into a pGEX1 vector to create plasmid pGEX1.DmC, which codes for a glutathione-*S*-transferase fusion protein (GST.

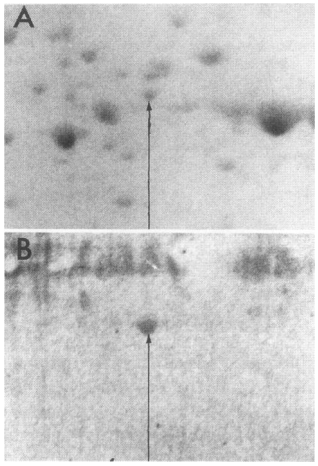

FIG. 4. Anti-$b_{6.1}$ specifically reacts with protein $b_{6.1}$, as identified by mobility on 2D gels. (A) Ovary proteins were separated by 2D gel electrophoresis and blotted to Immobilon-P membrane. The blot was stained with Coomassie brilliant blue. To conserve space, only a portion of the gel is shown. This portion extends from approximately pH 5.5 (left) to pH 6.5 (right) and molecular mass 65 kDa (top) to 35 kDa (bottom). The large, darkly staining spot on the left half of the panel is actin, and the series of two to three darkly staining spots at the right-hand edge of the panel are yolk proteins. Protein $b_{6.1}$ is indicated by the arrow. (B) The blot in panel A was destained, reacted with anti-$b_{6.1}$ and alkaline phosphatase-conjugated secondary antibody, and stained for alkaline phosphatase. Anti-$b_{6.1}$ reacted with protein $b_{6.1}$ (indicated by the arrow) and with no other spot. The background staining seen at the top of the panel is sporadically seen on 2D Western blots and appears to be nonspecific background.

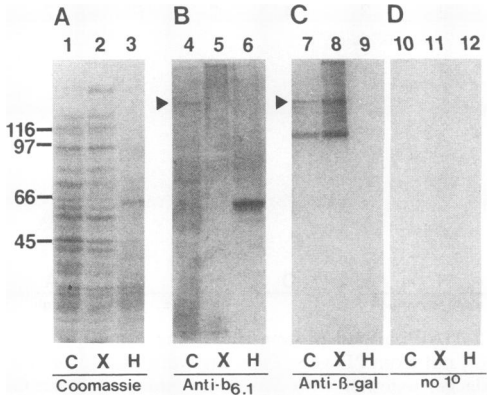

FIG. 5. Anti-$b_{6.1}$ specifically reacts with the fusion protein encoded by λgt11.DmC. Bacterial lysate proteins and HAP-purified protein $b_{6.1}$ were analyzed by 1D gel electrophoresis on a 9% acrylamide gel and transferred to Immobilon-P membrane. Lanes C contain proteins from a lysate of bacteria infected with λgt11.DmC. Lanes X contain proteins from a lysate of bacteria infected with a different bacteriophage (λgt11.DmX) in the same expression vector library. Lanes H contain HAP-purified protein $b_{6.1}$. (A) A section of this membrane was stained with Coomassie brilliant blue. (B) Another membrane section was reacted with anti-$b_{6.1}$ and alkaline phosphatase-conjugated secondary antibody and then stained for alkaline phosphatase. (C) Another section was reacted with anti-β-galactosidase antibody and alkaline phosphatase-conjugated secondary antibody and then stained for alkaline phosphatase. (D) Another section was not reacted with a primary antibody but was reacted with alkaline phosphatase-conjugated secondary antibody and then stained for alkaline phosphatase. Note that lysate from λgt11.DmC-infected bacteria contains a 150-kDa fusion protein that reacts with anti-$b_{6.1}$ (lane 4) and also with anti-β-galactosidase antibody (lane 7, arrowhead). λgt11.DmX-infected bacterial lysate reacts with anti-β-galactosidase antibody but does not react with anti-$b_{6.1}$, showing that anti-$b_{6.1}$ reacts with the *Drosophila* portion of λgt11.DmC fusion protein and not with the β-galactosidase portion. Anti-$b_{6.1}$ does not react with the *Drosophila* protein encoded by λgt11.DmX, indicating that anti-$b_{6.1}$ shows specificity for the protein encoded by λgt11.DmC.

DmCp). Anti-$b_{6.1}$ reacts with a single band at 55 kDa in a lysate of bacteria infected with pGEX1.DmC (Fig. 6), confirming that the pGEX1.DmC encodes an epitope recognized by anti-$b_{6.1}$. A rabbit antiserum to GST.DmCp was raised. This antiserum (anti-GST.DmCp) was affinity purified on a GST.DmCp-glutathione column. The affinity-purified anti-GST.DmCp reacts in a highly specific manner with HAP protein $b_{6.1}$ on 1D Western blots (Fig. 6). Anti-GST.DmCp reacts with only one spot on a 2D Western blot of total ovary proteins. This spot had the same molecular weight and isoelectric point as protein $b_{6.1}$.

Since a slight misalignment of the Coomassie blue-stained blot relative to the antibody-stained blot could lead to misidentification of protein $b_{6.1}$ on the blot, another experiment was devised to unequivocally identify protein $b_{6.1}$ on these blots. This experiment took advantage of the finding that protein $b_{6.1}$ has only one isoform in wild-type tissue but two in *quartet* homozygous tissue (11–13). These two isoforms are readily resolved by 2D gel electrophoresis. Thus, for this experiment, ovary proteins from *quartet* homozygous females were separated by 2D gel electrophoresis and transferred to an Immobilon-P membrane. The proteins on this membrane were reacted with anti-GST.DmCp. This antiserum reacted with one spot in a blot of wild-type ovary proteins and with two spots in the *quartet* ovary proteins (Fig. 7). These two spots correspond exactly in molecular weight and isoelectric point to the two protein $b_{6.1}$ isoforms found in *quartet* tissue. Therefore, the spots which reacted with anti-GST.DmCp are unequivocally identified as protein $b_{6.1}$. We conclude that GST-DmCp shares an epitope with protein $b_{6.1}$.

Thus, a mouse antiserum to HAP protein $b_{6.1}$ cross-reacts with β-gal.DmCp fusion protein and a rabbit antiserum to GST.DmCp fusion protein cross-reacts with HAP protein $b_{6.1}$. These results indicate that HAP protein $b_{6.1}$ and the protein encoded by the cDNA insert in λgt11.DmC and in pGEX1.DmC share an epitope and that this cDNA is likely to code for protein $b_{6.1}$.

To test this idea, we determined the nucleotide sequence of this cDNA. The insert λgt11.DmC was used to screen a λgt10 *Drosophila* adult female cDNA library. A complete 1.6-kb cDNA insert was obtained (λgt10.Dm237). The cDNA inserts in λgt11.DmC and in λgt10.Dm237 were completely sequenced (Fig. 8). To confirm that this cDNA sequence codes for protein $b_{6.1}$, we cleaved HAP protein $b_{6.1}$ with CNBr and determined the amino acid sequences of four of the resulting peptides. The sequences of all four peptides, representing a total of 98 residues, matched the conceptual translation of the nucleotide sequence of the cDNA inserts in λgt11.DmC and λgt10.Dm237. The amino acid sequences of these four peptides are underlined in Fig. 8. We conclude that λgt11.DmC and λgt10.Dm237 contain cDNAs which code for protein $b_{6.1}$.

Protein $b_{6.1}$ is a *Drosophila* homolog of bovine *smg* p25a GDP dissociation inhibitor. The cDNA sequence encoding protein $b_{6.1}$ was used to search the GenBank database by

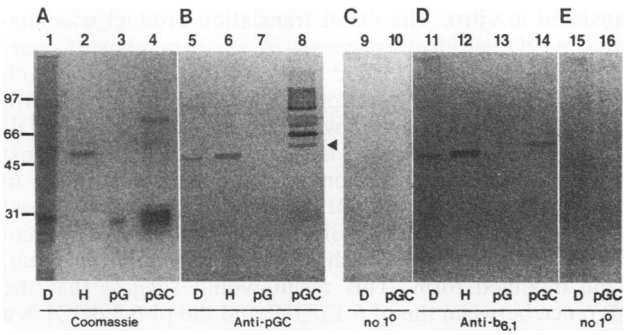

FIG. 6. Affinity-purified anti-GST.DmCp antibody reacts with protein $b_{6.1}$. Fly proteins and bacterial lysate proteins were separated by 1D gel electrophoresis and blotted to Immobilon-P membrane. Panel A was stained with Coomassie brilliant blue. Panel B was reacted with an affinity-purified anti-GST.DmCp rabbit antibody and with an alkaline phosphatase-conjugated anti-rabbit secondary antibody and stained for alkaline phosphatase. Panel C was reacted with alkaline phosphatase-conjugated anti-rabbit secondary antibody and stained for alkaline phosphatase. Panel D was reacted with mouse anti-$b_{6.1}$ and with an alkaline phosphatase-conjugated anti-mouse secondary antibody and stained for alkaline phosphatase. Panel E was reacted with alkaline phosphatase-conjugated anti-mouse secondary antibody and stained for alkaline phosphatase. Lanes: D, DEAE-pooled fly proteins (Fig. 1A); H, HAP protein $b_{6.1}$; pG, affinity-purified proteins from a pGEX1 bacterial lysate in which expression of glutathione-*S*-transferase was induced (pGEX1 has no inserted fly DNA; proteins were bound to a column of oxidized glutathione and eluted with reduced glutathione); pGC, affinity-purified proteins from a bacterial lysate of bacteria containing the plasmid pGEX1.DmC, which contains the fly cDNA 0.9-kb insert from λgt11.DmC (proteins were bound to a column of oxidized glutathione and eluted with reduced glutathione). The band at 55 kDa is the DmC-glutathione-*S*-transferase fusion protein, since only this protein cross-reacts with anti-$b_{6.1}$ (lane 14). The proteins in the 60- to 120-kDa region are induced along with glutathine-*S*-transferase in pGEX1.DmC and bind to and elute from the glutathione affinity column. These proteins do not react with anti-$b_{6.1}$, which is a polyclonal serum that reacts specifically with HAP protein $b_{6.1}$, and so these are not variant fusion proteins that contain segments of protein $b_{6.1}$. They most probably are bacterial proteins which are induced in bacteria infected with pGEX1.DmC, possibly by the fusion protein itself. The affinity-purified anti-GST.DmCp (anti-pGC) reacts specifically with protein $b_{6.1}$ in the DEAE pool (lane 5), with HAP protein $b_{6.1}$ (lane 6), and also with a 55-kDa protein in the affinity-purified pGEX1.DmC extract (lane 8, arrowhead), indicating that the peptides encoded by the cDNAs in pGEX1.DmC and protein $b_{6.1}$ share at least one epitope.

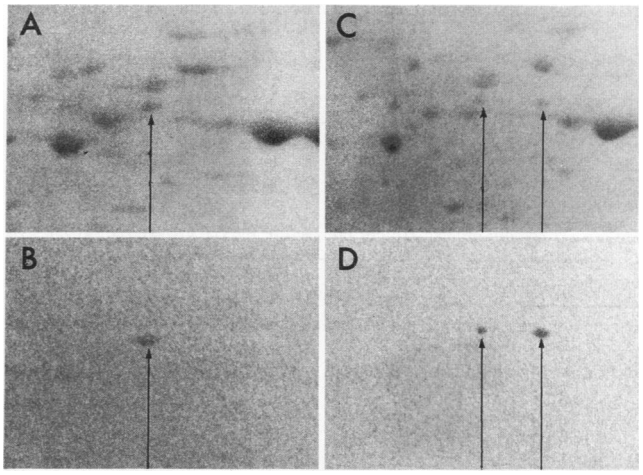

FIG. 7. Affinity-purified anti-GST.DmCp antibody reacts with protein $b_{6.1}$ in 2D gels of ovary proteins. (A) Wild-type ovary proteins were separated on 2D gels, transferred to Immobilon-P membrane, and stained with Coomassie brilliant blue. The region of the gel shown in this figure is the same as that shown in Fig. 4. The arrow points to protein $b_{6.1}$. (B) The blot of wild-type ovary proteins shown in panel A was destained and reacted with anti-GST.DmCp and then with alkaline phosphatase-conjugated anti-rabbit secondary antibody and stained for alkaline phosphatase. The arrow points to protein $b_{6.1}$. This is the only spot that stains on the entire 2D gel. (C) Ovary proteins from *quartet*^{RW630} flies that had been kept at 27°C for 3 days. These proteins were separated on a 2D gel, transferred to an Immobilon-P membrane, and stained with Coomassie brilliant blue. The arrows point to the wild-type (left) and mutant (right) forms of protein $b_{6.1}$. (D) The blot of mutant ovary proteins shown in panel B was destained and reacted with anti-GST.DmCp and then with alkaline phosphatase-conjugated anti-rabbit secondary antibody and stained for alkaline phosphatase. The arrows point to the wild-type (left) and mutant (right) forms of protein $b_{6.1}$. These are the only two proteins that stain on the entire 2D gel. This indicates that anti-GST.DmCp reacts specifically with protein $b_{6.1}$.

using the FASTA program (30). A single match was found. This match was to bovine *smg* p25a GDI (28). With the ALIGN program, the nucleotide sequence shows 66% identity to the sequence of bovine *smg* p25a GDI. With BESTFIT, the conceptual translation of the protein $b_{6.1}$ sequence has 68% identity and 81% similarity at the amino acid level to bovine *smg* p25a GDI (Fig. 9). Because of this strong homology, we propose that protein $b_{6.1}$ should be named dGDI. The homology between bovine *smg* p25a GDI and dGDI extends throughout the length of the protein, with only two regions showing divergence. These two regions are in the middle of the protein from amino acid residues 156 to 182 and at the extreme -COOH end.

dGDI is encoded by a single-copy gene in *D. melanogaster*. When λgt11.DmC cDNA was hybridized to polytene chromosomes, a single band at 30B showed hybridization. Since the polytene chromosome location of *quartet* is 92AB, it is clear that dGDI is not encoded by *quartet*. Hybridization of λgt11.DmC cDNA to restriction digests of *Drosophila* genomic DNA at both high and low stringency showed only one or two bands per restriction digest, also indicating that *dGDI* is a single-copy gene and is not a member of a highly homologous family of *Drosophila* genes.

Chemical nature of the modification. Analysis of the *dGDI* sequence by using the MOTIFS program of the University of Wisconsin Genetics Computer Group sequence analysis programs indicated 14 potential phosphorylation sites and 2 potential amidation sites. No other posttranslational modification sites were found by this program.

Previous experiments indicated that inorganic $^{32}PO_4^{3-}$ and $^{35}SO_4^{2-}$ were not incorporated into dGDI when wild type *Drosophila* ovaries were labeled in vitro (13). Because the sequence indicated numerous possible phosphorylation sites, several more experiments were performed to test the possibility that the quartet-affected modification of dGDI is a phosphorylation. One of the potential phosphorylation consensus sequences in dGDI is a tyrosine. Two different antibodies to phosphotyrosine were reacted with a Western blot of purified dGDI. No reaction above background was observed, indicating that it is unlikely that dGDI undergoes tyrosine phosphorylation.

In a second series of experiments, dGDI was treated with phosphatase to see whether this would result in a shift in isoelectric point similar to the quartet shift. The treated protein was analyzed by 2D gel electrophoresis, with un-

```
AAAAAAAATATATAAATTACTGTGATTGCAATATATAATATAGTGTGATCCAAT ATG GAT GAG GAA TAC   69
                                                        M  D  E  E  Y     5

GAT GTC GAT GTG CTA GGA ACC GGG CTC AAG GAG TGC ATC CTC AGC GGG ATA ATG CTG  126
 D  V  D  V  L  G  T  G  L  K  E  C  I  L  S  G  I  M  L                   24

TCC GTG TCC GGC AAG AAG GTT TTG CAT ATT GAT CGA AAC AAG TAC TAC GGC GGC GAG  183
 S  V  S  G  K  K  V  L  H  I  D  R  N  K  Y  Y  G  G  E                   43

TCC GCT TCG ATA ACG CCG CTG GAG GAG CTC TTC CAG CGC TAC CGG ACT GGA GCC GCC  240
 S  A  S  I  T  P  L  E  E  L  F  Q  R  Y  R  T  G  A  A                   62

CGG CCA CGA TTT GGG CGT GGC CGC GAC TGG AAC GTG GAC CTG ATC CCT AAG TTC CTA  297
 R  P  R  F  G  R  G  R  D  W  N  V  D  L  I  P  K  F  L                   81

ATG GCC AAT GGC CAG CTG GTC AAG CTG CTG ATC CAC ACG GGC GTC ACC CGC TAT CTG  354
 M  A  N  G  Q  L  V  K  L  L  I  H  T  G  V  T  R  Y  L                  100

GAG TTC AAG TCC ATC GAG GGC AGC TAC GTT TAC AAG GGC GGC AAG ATA GCC AAG GTG  411
 E  F  K  S  I  E  G  S  Y  V  Y  K  G  G  K  I  A  K  V                  119

CCG GTG GAC CAA AAG GAG GCC CTG GCA TCC GAT CTC ATG GGT ATG TTC GAG AAG CGT  468
 P  V  D  Q  K  E  A  L  A  S  D  L  M  G  M  F  E  K  R                  138

CGC TTC CGG AAC TTC CTC ATC TAC GTG CAG GAT TTC CGA GAA GAT GAC CCC AAG ACC  525
 R  F  R  N  F  L  I  Y  V  Q  D  F  R  E  D  D  P  K  T                  157

TGG AAG GAC TTT GAC CCC ACC AAG GCC AAC ATG CAG GGT CTG TAC GAC AAG TTC GGA  582
 W  K  D  F  D  P  T  K  A  N  M  Q  G  L  Y  D  K  F  G                  176

CTG GAC AAG AAC ACG CAG GAC TTC ACC GGC CAC GCC CTG GCC CTT TTC CGC GAC GAT  639
 L  D  K  N  T  Q  D  F  T  G  H  A  L  A  L  F  R  D  D                  195

GAG TAT CTG AAC GAG CCG GCC GTT AAC ACC ATC CGG CGG ATT AAG CTC TAC TCC GAT  696
 E  Y  L  N  E  P  A  V  N  T  I  R  R  I  K  L  Y  S  D                  214

TCG CTG GCG CGT TAC GGC AAG TCG CCC TAC CTT TAT CCC ATG TAC GGC CTG GGT GAG  753
 S  L  A  R  Y  G  K  S  P  Y  L  Y  P  M  Y  G  L  G  E                  233

CTG CCC CAG GGA TTC GCA CGC TTG TCG GCC ATC TAC GGC GGC ACC TAT ATG CTG GAC  810
 L  P  Q  G  F  A  R  L  S  A  I  Y  G  G  T  Y  M  L  D                  252

AAG CCC ATC GAC GAG ATT GTC CTC GGC GAG GGC GGC AAG GTG GTG GGA GTG CGC TCC  867
 K  P  I  D  E  I  V  L  G  E  G  G  K  V  V  G  V  R  S                  271

GGC GAA GAG GTC GCC AAG TGC AAG CAG GTC TAC TGC GAT CCC AGC TAC GTG CCG AGA  924
 G  E  E  V  A  K  C  K  Q  V  Y  C  D  P  S  Y  V  P  R                  290

AGG TTG CGC AAG CGT GGC AAG GTG ATT CGC TGC ATT TGC ATT CAG GAC CAT CCA GGT  981
 R  L  R  K  R  G  K  V  I  R  C  I  C  I  Q  D  H  P  G                  309

GCC AGC ACC AAG GAT GGT CTC TCC ACG CAG ATT ATC ATT CCA CAA AAG CAG GTT GGC 1038
 A  S  T  K  D  G  L  S  T  Q  I  I  I  P  Q  K  Q  V  G                  328

CGC AAG TCG GAC ATC TAT GTA TCG CTT GTG AGC TCC ACT CAT CAG GTG GCC GCC AAG 1095
 R  K  S  D  I  Y  V  S  L  V  S  S  T  H  Q  V  A  A  K                  347

GGT TGG TTC GTA GGC ATG GTC TCG ACC ACC GTT GAG ACC GAG AAC CCG GAG GTG GAG 1152
 G  W  F  V  G  M  V  S  T  T  V  E  T  E  N  P  E  V  E                  366

ATC AAG CCT GGC TTG GAC TTG CTG GAG CCG ATC GCA CAA AAG TTT GTG ACC ATT TCG 1209
 I  K  P  G  L  D  L  L  E  P  I  A  Q  K  F  V  T  I  S                  385

GAT TAC TTG GAG CCG ATC GAT GAT GGA TCC GAG TCT CAA ATC TTT ATT TCG GAG TCT 1266
 D  Y  L  E  P  I  D  D  G  S  E  S  Q  I  F  I  S  E  S                  404

TAC GAT GCG ACC ACG CAC TTT GAG ACT ACT TGC TGG GAT GTG TTG AAC ATA TTC AAG 1323
 Y  D  A  T  T  H  F  E  T  T  C  W  D  V  L  N  I  F  K                  423

CGG GGC ACT GGC GAG ACG TTC GAC TTC TCC AAG GAT CAA GGC ACG AGT TGG GTG ACG 1380
 R  G  T  G  E  T  F  D  F  S  K  D  Q  G  T  S  W  V  T                  442

AGG AGC AGT AAA CGG GAA TGAAGGCCTCATCTGGTTATGGTGCATTTGGACAGCTCAACATCAGCCACA 1449
 R  S  S  K  R  E                                                         448

AACATCGTAGATCGTCTCAGCATGTCGTGGCTCAAACCTTAAAAAAAAAAAAAAAAAACCCAAGATAAGAAAACCCA 1524
AAATAAAAGCCCAAAAAAACTAAAAAAAAAAAAAAAACC                                   1563
```

FIG. 8. Sequence of protein $b_{6.1}$ cDNA. The complete nucleotide sequence of λgt10.Dm237 is shown. Underneath the nucleotide sequence is the conceptual translation of this sequence in the single-amino-acid code. The underlined residues indicate the four peptides of HAP protein $b_{6.1}$ that were sequenced. The amino acid sequences of these four peptides were completely identical to the conceptual translation of this cDNA except at residue 229. At this residue, amino acid sequence analysis gave leucine but the nucleotide sequence of the cDNA in λgt10.Dm237 and in λgt11.DmC codes for tyrosine. This could possibly represent a polymorphic site.

treated dGDI added to the sample to act as an internal marker on the same gel. Phosphatase-treated and control dGDI had exactly the same mobility, indicating that dGDI is probably not phosphorylated. Several minor contaminant proteins did shift in isoelectric point, indicating that the phosphatase was functional, a finding which was also confirmed by colorimetric assay of phosphatase activity.

A third series of experiments was designed to find whether the modification was acidic or basic. The dGDI complete cDNA was transcribed in vitro, and the transcript was translated in vitro. The dGDI translation product was analyzed by 2D gel electrophoresis. A small number of *quartet*^{RW630} ovaries were loaded as an internal marker for both isoforms of dGDI. It was found that most of the in vitro translated dGDI comigrated with the pI 6.1 isoform of dGDI, the more acidic of the two isoforms (Fig. 10). Since most posttranslational modifications work inefficiently in an in vitro translation system (6, 21, 33), this result would suggest that the pI 6.1 isoform of dGDI is the unmodified form and that the pI 6.2 isoform, which accumulates in *quartet* tissue, is the modified form. This result would suggest that the difference between the pI 6.1 dGDI and the pI 6.2 dGDI is a basic modification.

DISCUSSION

We report here a *Drosophila* homolog to bovine *smg* p25a GDI, a regulator of small GTPases of the *rab/SEC4/YPT1* family. Until now, only three GDIs have been purified: *smg* p25a GDI, *rho* GDI, and *rab11* GDI (42). *smg* p25a GDI has been shown to bind specifically to the *rab/SEC4/YPT1* family of GTP-binding proteins and not to proteins from other small GTPase families, such as *ras* and *rho* (38, 39). *rho* GDI is very different from *smg* p25a GDI: it is only about half the size of *smg* p25a GDI (44) and does not show any homology to *smg* p25a GDI at either the nucleotide or amino acid level (18). Moreover, *rho* GDI has been reported to have two functions. In addition to acting as a GDI specifically on *rho* (and not on *ras* or *smg* p25a), it is part of an activating complex for NADPH oxidase (1). Rat *rab11* GDI is very similar to bovine *smg* p25a GDI (45). The limited sequence information indicates that of 83 amino acids sequenced, only 2 differ. However, bovine *smg* p24 GDI is active on *rab11* and not on *smg* p25a, whereas rat *rab11* GDI is active on both *rab11* and *smg* p25a. It is not clear whether this represents two distinct classes of *rab* GDIs or whether the incomplete reactivity of rat *rab11* GDI on bovine *smg* p25a is due to species specificity.

dGDI is a single-copy gene, indicating that *Drosophila* does not appear to have a family of closely related *rab* GDIs. Vertebrates have at least 12 *rab* GTPases, and yeasts have 2 (reviewed in reference 3). In *D. melanogaster*, one *rab* gene has been identified (a homolog of *rab3A* [24]), and it is likely that *D. melanogaster* also has multiple *rab* GTPases. Thus, the GDI encoded by the single *dGDI* gene in *D. melanogaster* may be active on multiple *rab* gene products which act at different points in the secretion and endocytosis pathways. Regulation of GDI function could be a global control point for vesicular transport and could provide a mechanism for coordinating the different steps in vesicular transport.

The accumulation of dGDI in the more basic isoform in quartet tissue suggests possible control of GDI function by posttranslational modification. Information on the chemical nature of the modification could prove useful in testing this hypothesis. However, despite considerable effort, the chemical nature of the *quartet*-affected modification of dGDI remains unknown. Although the sequence indicates multiple possible phosphorylation sites, dGDI does not label with $^{32}PO_4^{3-}$ in vivo (13), does not change charge when treated with phosphatase, and does not react with anti-phosphotyrosine. Thus, phosphorylation appears unlikely. Experiments testing sulfation, acetylation, and myristylation have also given negative results (13, 26). Experiments are in progress to purify both isoforms of dGDI in order to allow

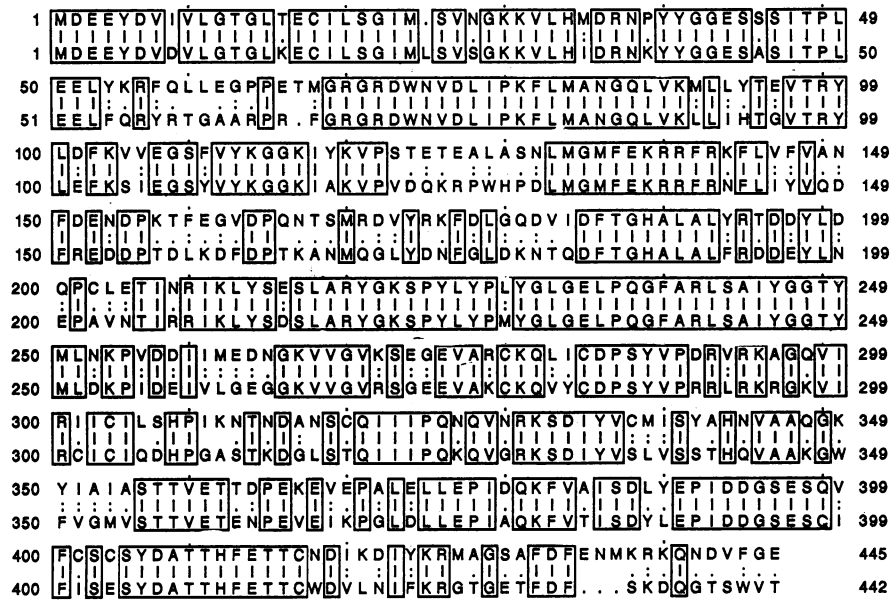

FIG. 9. Protein $b_{6.1}$ is homologous to bovine *smg* p25a GDI. Alignment of the conceptual translation of *dGDI* and of bovine *smg* p25a GDI (26) by using the BESTFIT program. The sequences share 68% identity and 81% similarity. Regions of identity are boxed.

more detailed chemical analysis and to test the functionality of both isoforms in in vitro assays.

In vitro translation of dGDI gives a product that consists almost entirely of the more acidic (pI 6.1) isoform. Since most posttranslational modifications work poorly, if at all, in an in vitro translation system (6, 21, 33), this result would suggest that the pI 6.1 dGDI isoform is the unmodified isoform and that it undergoes a basic modification and accumulates in *quartet* homozygous tissue. However, since genetic data demonstrate conclusively that all five mutations of *quartet* that have been examined are loss-of-function mutations (11, 12, 31), it seems unlikely that *quartet* mutations create a novel modifying activity. It could be that a basic modification inactivates dGDI and that the wild-type *quartet* gene product removes the basic modification and reactivates dGDI (Fig. 11). This cycle of modification and demodification may be essential for dGDI to bind and then release *rab* GTPases. It may be that the *quartet* gene product is involved in a cycle of modification and demodification which regulates dGDI function (Fig. 11).

There is a very tight correlation between the shift in dGDI and the *quartet* developmental phenotype. Five different *quartet* alleles, in different genetic backgrounds, have been examined, and all five show the shift in dGDI (12). This indicates that the pI 6.2 dGDI isoform is not a background

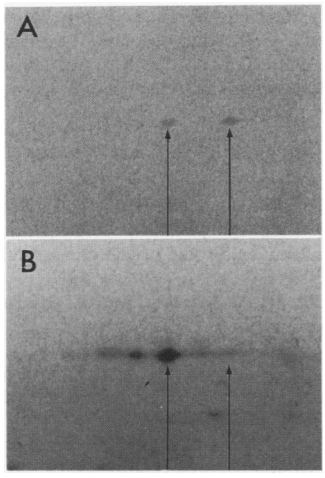

FIG. 10. In vitro-translated dGDI comigrates with the pI 6.1 isoform of dGDI. (A) Western blot. T7 polymerase was used to make a dGDI transcript from pBS.237. The transcript was translated in vitro in the presence of [^{35}S]methionine. This translation product was loaded onto a 2D gel together with several ovaries from *quartet*^{RW630} females that had been kept at the restrictive temperature (27°C) for 2 days. The proteins on this gel were transferred to Immobilon-P membrane and stained with anti-native dGDI. The two arrows indicate the pI 6.1 (left) and the pI 6.2 (right) dGDI isoforms. (B) Autoradiograph of the blot shown in panel A. dGDI that is translated in vitro consists almost entirely of the pI 6.1 isoform (left arrow). Very little of the pI 6.2 dGDI isoform (right arrow) is found.

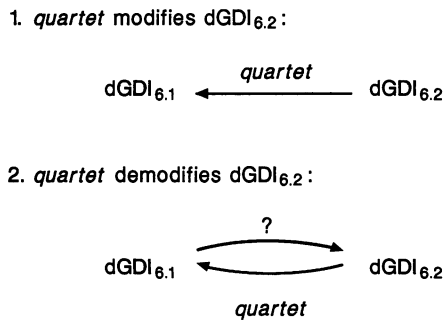

FIG. 11. Possible roles of *quartet* in dGDI function. Role 1: The wild-type *quartet* gene product could perform an acidic modification of pI 6.2 dGDI which converts dGDI from an inactive to an active form. Role 2: An unknown gene product could perform a basic modification of $dGDI_{6.1}$, which inactivates dGDI and possibly allows it to separate from the *rab* GTPase. The wild-type *quartet* gene product could remove this basic modification and restore dGDI activity.

polymorphism. The amount of dGDI shifted is closely correlated with the severity of the phenotype. Furthermore, in the temperature-sensitive *quartet* allele, both the shift and the developmental phenotype are temperature sensitive (11). Such close correlation between dGDI shift and developmental phenotype suggest that part of the *quartet* phenotype could be due to improper dGDI function or regulation. If this were true, one would predict that the *quartet* phenotype would involve defects in vesicular transport.

Three aspects of the *quartet* phenotype are consistent with defects in secretion or endocytosis. First, $quartet^{RW630}$ homozygous females secrete defective chorions and vitelline membranes at the restrictive temperature (13). These membranes are secreted by the follicle cells of the ovary in late oogenesis and surround the oocyte. Eggs produced by $quartet^{RW630}$ females after 24 h or more at the restrictive temperature have thin, translucent chorions and vitelline membranes, which allow the embryo to desiccate much more rapidly than normal. These observations point to a secretion defect in $quartet^{RW630}$ follicles.

A second aspect of the *quartet* phenotype consistent with a defect in vesicular transport is the accumulation of large vesicles in the brains of *quartet* homozygous larvae, giving the brain a spongy appearance in histological sections (10a). This is very similar to the larval brain phenotype of the *Drosophila* mutant *awd* (16). *awd* codes for a nucleoside diphosphate kinase and so could be important for the conversion of GDP to GTP (4). An allele of *awd* ($awd^{K\text{-}pn}$) has a well-established interaction with *pn*, a GAP homolog (5, 43). Thus, it is possible that both *awd* and quartet affect small GTPase function in vesicular transport. A block in vesicular transport in the larval brain could lead to the accumulation of vesicles seen in the larval brains of *awd* and *quartet* homozygotes.

A third aspect of the *quartet* phenotype which is consistent with a defect in vesicular transport is the lack of neuromuscular coordination seen in $quartet^{NC806}$ homozygotes (31). $quartet^{NC806}$ is a very mild allele of *quartet*, and these homozygotes often live to the pharate adult stage but have difficulty crawling out of the pupal case at eclosion. If they are assisted in eclosion, these flies cannot coordinate their movements and do not walk or fly normally. In another *Drosophila* mutant, *shibire*, defects in neural function are associated with defects in endocytosis (34).

It is more difficult to attribute the mitotic defects in quartet to defects in the known functions of *rab* GTPases and of GDIs. Mitotic defects are observed in *quartet* homozygotes at two points in the life cycle. One developmental stage at which mitotic defects are seen is in embryos produced by $quartet^{RW630}$ homozygous females at restrictive temperature (47). These embryos show incomplete chromosome separation at the syncytial blastoderm stage. This could be due to a defective mitotic spindle, improper chromosome condensation, or incomplete DNA synthesis. Since most zygotic transcription in the *Drosophila* embryo does not begin until the cellular blastoderm stage, all the materials needed for the early embryonic mitotic activity must be packed into the egg during oogenesis. Defective secretion or endocytosis could impair this process. Lack of a maternally supplied product needed for spindle function, chromosome condensation, or DNA synthesis could lead to the observed mitotic defects. Indeed, homozygous $quartet^{RW630}$ females must be exposed to a restrictive temperature for at least 1 day before a defect is seen in the embryos they produce (11). Furthermore, if these affected embryos are kept at a permissive temperature, the same range of defects are observed. These observations are consistent with a role for *quartet* in a process in oogenesis, such as in vesicular transport in the nurse cell-oocyte complex.

The second point of the life cycle at which mitotic defects are observed in *quartet* homozygotes is during late third instar. A reduced mitotic index with an elevated frequency of abnormal mitotic figures has been seen in the larval brains of four *quartet* alleles (31, 47). In the abnormal mitotic figures, common abnormalities seen are fragmented chromosomes and incompletely condensed chromosomes. It is more difficult to attribute these mitotic defects to defects in secretion and endocytosis. The *rab* family of small GTPases has not been implicated directly in other kinds of intracellular movement, such as chromosome movement, although a subset of *rab* GTPases is phosphorylated in concert with the mitotic cycle (2). The final test of the role of dGDI in the *quartet* phenotype, in vesicular transport, and in mitosis will be the isolation of dGDI mutants and examination of their phenotype.

ACKNOWLEDGMENTS

We are grateful to R. Jones for expert assistance with in situ hybridizations. Human lymphocytes were provided by S. Bland and D. S. Gerhard.

This research was supported by a Biomedical Research Support Group grant from NIH to Washington University, by the Lucille P. Markey Charitable Trust, and by the National Science Foundation (grant DCB9205697 to C.M.C.).

REFERENCES

1. **Abo, A., E. Pick, A. Hall, N. Totty, C. G. Teahan, and A. W. Segal.** 1991. Activation of the NADPH oxidase involves the small GTPase $p21^{rac1}$. Nature (London) **353**:668–670.
2. **Bailly, E., M. McCaffrey, N. Touchot, A. Zahraoui, B. Goud, and M. Bornens.** 1991. Phosphorylation of two small GTPases of the Rab family by $p34^{cdc2}$. Nature (London) **350**:715–718.
3. **Balch, W. E.** 1990. Small GTP-binding proteins in vesicular transport. Trends Biochem. Sci. **15**:473–476.
4. **Biggs, J., E. Hersperger, P. S. Steeg, L. A. Liotta, and A. Shearn.** 1990. A *Drosophila* gene that is homologous to a mammalian gene associated with tumor metastasis codes for a nucleoside diphosphate kinase. Cell **63**:933–940.
5. **Biggs, J., N. Tripoulas, E. Hersperger, C. Dearolf, and A. Shearn.** 1988. Analysis of the lethal interaction between the *prune* and *Killer of prune* mutations of *Drosophila*. Genes Dev. **2**:1333–1343.
6. **Borner, C., I. Filipuzzi, M. Wartmann, U. Eppenberger, and D. Fabbro.** 1989. Biosynthesis and post-translational modifications of protein kinase C in human breast cancer cells. J. Biol. Chem. **264**:13902–13909.
7. **Bourne, H. R., D. A. Sanders, and F. McCormick.** 1990. The GTPase superfamily: a conserved switch for diverse cell functions. Nature (London) **348**:125–132.
8. **Bourne, H. R., D. A. Sanders, and F. McCormick.** 1991. The GTPase superfamily: conserved structure and molecular mechanism. Nature (London) **349**:117–127.
9. **Bradford, M. M.** 1976. A rapid and sensitive method for the quantitation of microgram quantities of protein utilizing the principle of protein-dye binding. Anal. Biochem. **86**:142–146.
10. **Charbonneau, H.** 1989. Strategies for obtaining partial amino acid sequence data from small quantities (<5nmol) of pure or partially pure protein, p. 24–30. In P. T. Matsudaira (ed.), A practical guide to protein and peptide purification for microsequencing. Academic Press, Inc., New York.

10a. **Cheney, C. M.** Unpublished data.

11. **Cheney, C. M., and T. J. Lang.** 1986. Defects in protein modification precede developmental defects in $I(3)c21R^{RW630}$, a temperature-sensitive *Drosophila* developmental mutation. Dev. Biol. **114**:34–41.
12. **Cheney, C. M., and T. J. Lang.** 1988. Developmental and

protein modification defects caused by mutations in the *Drosophila* gene, *I(3)c21R*. Dev. Biol. **130**:551–557.
13. **Cheney, C. M., K. G. Miller, T. J. Lang, and A. Shearn.** 1984. Specific protein modifications are altered in a temperature-sensitive *Drosophila* developmental mutant. Proc. Natl. Acad. Sci. USA **81**:6422–6426.
14. **Cheney, C. M., and A. Shearn.** 1983. Developmental regulation of *Drosophila* imaginal disc proteins: synthesis of heat shock proteins under non-heat-shock conditions. Dev. Biol. **95**:325–330.
15. **Cleveland, D. W., S. G. Fischer, M. W. Kirschner, and U. K. Laemmli.** 1977. Peptide mapping by limited proteolysis in sodium dodecyl sulfate and analysis by gel electrophoresis. J. Biol. Chem. **252**:1102–1106.
16. **Dearolf, C. R., E. Hersperger, and A. Shearn.** 1988. Developmental consequences of awd^{b3}, a cell-autonomous lethal mutation of *Drosophila* induced by hybrid dysgenesis. Dev. Biol. **129**:159–168.
17. **Feinberg, A. P., and B. Vogelstein.** 1984. A technique for radiolabeling DNA restriction endonuclease fragments to high specific activity. Anal. Biochem. **137**:266–267.
18. **Fukumoto, Y., K. Kaibucki, Y. Hori, H. Fujioka, S. Araki, T. Ueda, A. Kikuchi, and Y. Takai.** 1990. Molecular cloning and characterization of a novel type of regulatory protein (GDI) for the *rho* proteins, *ras* p21-like small GTP binding proteins. Oncogene **5**:1321–1328.
19. **Fyrberg, E. A., and J. J. Donady.** 1979. Actin heterogeneity in primary embryonic culture cells from *Drosophila melanogaster*. Dev. Biol. **68**:487–502.
20. **Hall, A.** 1990. The cellular functions of small GTPases. Science **249**:635–640.
21. **Hancock, J. F., K. Cadwallader, and C. J. Marshall.** 1991. Methylation and proteolysis are essential for efficient membrane binding of prenylated $p21^{K\text{-}ras}$. EMBO J. **10**:641–646.
22. **Harlow, E., and D. Lane.** 1988. Antibodies: a laboratory manual. Cold Spring Harbor Laboratory, Cold Spring Harbor, N.Y.
23. **Johnson-Schlitz, D., and J. K. Lim.** 1987. Cytogenetics of *Notch* mutations arising in the unstable X chromosome Uc of *Drosophila melanogaster*. Genetics **115**:701–709.
24. **Johnston, P. A., B. T. Archer III, K. Robinson, G. A. Mignery, R. Joan, and T. C. Sudhof.** 1991. rab3A attachment to the synaptic vesicle membrane mediated by a conserved polyisoprenylated carboxy-terminal sequence. Neuron **7**:101–109.
25. **Laemmli, U. K.** 1970. Cleavage of structural proteins during the assembly of the head of bacteriophage T4. Nature (London) **227**:680–685.
26. **Lang, T. J., J. E. Zahner, and C. M. Cheney.** Unpublished data.
27. **Langer-Safer, P. R., M. Levine, and D. C. Ward.** 1982. Immunological method for mapping genes on *Drosophila* polytene chromosomes. Proc. Natl. Acad. Sci. USA **79**:4381–4385.
28. **Matsui, Y., A. Kikuchi, S. Araki, Y. Hata, J. Kondo, Y. Teranishi, and Y. Takai.** 1990. Molecular cloning and characterization of a novel type of regulatory protein (GDI) for *smg* p25A, a *ras* p21-like GTP-binding protein. Mol. Cell. Biol. **10**:4116–4122.
29. **O'Farrell, P. H.** 1975. High resolution two-dimensional electrophoresis of proteins. J. Biol. Chem. **250**:4007–4021.
30. **Pearson, W. R., and D. J. Lipman.** 1988. Improved tools for biological sequence comparison. Proc. Natl. Acad. Sci. USA **85**:2444–2448.
31. **Pentz, E. S.** 1979. Mutational dissection of development: analysis of mutations of the *c21R* locus which cause abnormal imaginal disc development in *Drosophila melanogaster*. Ph.D. dissertation. The Johns Hopkins University, Baltimore, Md.
32. **Pentz, E. S., and A. Shearn.** 1977. Analysis of the autonomy of imaginal disc defects in a small-disc mutant of *Drosophila melanogaster*. Dev. Biol. **70**:149–170.
33. **Pollard, K. M., E. K. L. Chan, B. J. Grant, K. F. Sullivan, E. M. Tan, and C. A. Glass.** 1990. In vitro posttranslational modification of lamin B cloned from a human T-cell line. Mol. Cell. Biol. **10**:2164–2175.
34. **Poodry, C. A.** 1990. *shibire*, a neurogenic mutant of *Drosophila*. Dev. Biol. **138**:464–472.
35. **Ruggieri, R., and F. McCormick.** 1991. Ras and the *awd* couple. Nature (London) **353**:390–391.
36. **Sambrook, J., E. F. Fritsch, and T. Maniatis.** 1989. Molecular cloning: a laboratory manual, 2nd ed. Cold Spring Harbor Laboratory, Cold Spring Harbor, N.Y.
37. **Sanger, F., S. Nicklen, and A. R. Coulson.** 1977. DNA sequencing with chain-terminating inhibitors. Proc. Natl. Acad. Sci. USA **74**:5463–5467.
38. **Sasaki, T., K. Kaibuchi, A. K. Kabcenell, P. J. Novick, and Y. Takai.** 1991. A mammalian inhibitory GDP/GTP exchange protein (GDP dissociation inhibitor) for *smg* p25A is active on the yeast SEC4 protein. Mol. Cell. Biol. **11**:2909–2912.
39. **Sasaki, T., A. Kikuchi, S. Araki, Y. Hata, M. Isomura, S. Kuroda, and Y. Takai.** 1990. Purification and characterization from bovine brain cytosol of a protein that inhibits the dissociation of GDP from and the subsequent binding of GTP to *smg* p25A, a *ras* p21-like GTP-binding protein. J. Biol. Chem. **265**:2333–2337.
40. **Smith, D. B., and K. S. Johnson.** 1988. Single-step purification of polypeptides expressed in *Escherichia coli* as fusions with glutathione-S-transferase. Gene **67**:31–40.
41. **Southern, E. M.** 1975. Detection of specific sequences among DNA fragments separated by gel electrophoresis. J. Mol. Biol. **98**:503–517.
42. **Takai, Y., K. Kaibuchi, A. Kikuchi, and M. Kawata.** 1992. Small GTP-binding proteins. Int. Rev. Cytol. **133**:187–230.
43. **Teng, D. H. F., C. M. Engele, and T. R. Venkatesh.** 1991. A product of the *prune* locus of *Drosophila* is similar to mammalian GTPase-activating protein. Nature (London) **353**:437–440.
44. **Ueda, T., A. Kikuchi, N. Ohga, J. Yamamoto, and Y. Takai.** 1990. Purification and characterization from bovine brain cytosol of a novel regulatory protein inhibiting the dissociation of GDP from and the subsequent binding of GTP to *rhoB* p20, a *ras* p21-like GTP-binding protein. J. Biol. Chem. **265**:9373–9380.
45. **Ueda, T., Y. Takeyama, T. Ohmori, H. Ohyanagi, Y. Satoh, and Y. Takai.** 1991. Purification and characterization from rat liver cytosol of a GDP dissociation inhibitor (GDI) for liver 24K G, a *ras* p21-like GTP-binding protein, with properties similar to those of *smg* p25a GDI. Biochemistry **30**:909–917.
46. **Wang, L. L., and J. A. Spudich.** 1984. A 45,000-mol-wt protein from unfertilized sea urchin eggs severs actin filaments in a calcium-dependent manner and increases the steady-state concentration of nonfilamentous actin. J. Cell Biol. **99**:844–851.
47. **Zahner, J. E., and C. M. Cheney.** 1990. *quartet*: a *Drosophila* developmental mutation affecting chromosome separation in mitosis. Dev. Genet. **11**:27–40.